Report

Current Biology

Origins of slow growth on the crocodilian stem lineage

Highlights

- A new giant basal crocodylomorph ancestor shows slow growth rates
- Small, active, terrestrial early crocodylomorphs grew like living crocodilians
- Only slow-growing crocodylomorphs survived the End-Triassic mass extinction
- This differs from the fast-growing dinosaurs that lived alongside them

Authors

Jennifer Botha, Bailey M. Weiss, Kathleen Dollman, Paul M. Barrett, Roger B.J. Benson, Jonah N. Choiniere

Correspondence

jennifer.botha1@wits.ac.za

In brief

Living crocodilians grow slowly, contrasting with their ancestors, who grew rapidly. Botha et al. constrain the origin of this transition to the Late Triassic. Thus, crocodylomorphs already differed from their concurrent relatives (including dinosaurs), prior to the End-Triassic extinction, with only slow-growing crocodylomorphs surviving the event.

Botha et al., 2023, Current Biology *33*, 4261–4268
October 9, 2023
https://doi.org/10.1016/j.cub.2023.08.057

CellPress

Current Biology

CellPress

Report

Origins of slow growth on the crocodilian stem lineage

Jennifer Botha,[1,2,7,*] Bailey M. Weiss,[1,3] Kathleen Dollman,[1,4] Paul M. Barrett,[1,5] Roger B.J. Benson,[1,6] and Jonah N. Choiniere[1]

[1]Evolutionary Studies Institute, University of the Witwatersrand, Johannesburg 2050, South Africa
[2]GENUS: DSI-NRF Centre of Excellence in Palaeosciences, University of the Witwatersrand, Johannesburg 2050, South Africa
[3]School of Geosciences, University of the Witwatersrand, Johannesburg 2050, South Africa
[4]European Synchrotron and Radiation Facility, Experiments Division, Structure of Materials Group, BM18, Grenoble 38000, France
[5]Fossil Reptiles, Amphibians and Birds Section, Natural History Museum, Cromwell Road, London SW7 5BD, UK
[6]Division of Paleontology, American Museum of Natural History, New York, NY 10024, USA
[7]Lead contact
*Correspondence: jennifer.botha1@wits.ac.za
https://doi.org/10.1016/j.cub.2023.08.057

SUMMARY

Crocodilians grow slowly and have low metabolic rates similar to other living reptiles, but palaeohistology indicates that they evolved from an ancestor with higher growth rates.[1–5] It remains unclear when slow growth appeared in the clade due to the sparse data on key divergences among early Mesozoic members of their stem lineage. We present new osteohistological data from a broad sample of early crocodylomorphs, evaluated in a phylogenetic context alongside other pseudosuchians. We find that the transition to slow-growing bone types during mid-late ontogeny occurred around the origin of Crocodylomorpha during the Late Triassic. Earlier-diverging pseudosuchians had high maximum growth rates, as indicated by the presence of woven bone during middle and (sometimes) late ontogeny.[6–9] Large-bodied pseudosuchians in particular exhibit some of the fastest-growing bone types, giving evidence for prolonged, rapid growth. By contrast, early-branching crocodylomorphs, including a new large-bodied taxon, had slow maximum rates of bone deposition, as evidenced by the presence of predominantly parallel-fibered or lamellar bone tissue during middle-late ontogeny. Late Triassic crocodylomorphs show skeletal anatomy consistent with "active" terrestrial habits,[10–12] and their slow growth rates reject hypotheses linking this transition with sedentary, semi-aquatic lifestyles or sprawling posture. Faster-growing pseudosuchian lineages go extinct in the Triassic, whereas slow-growing crocodylomorphs do not. This contrasts with the Jurassic radiation of fast-growing dinosaurs on the bird-stem lineage,[13] suggesting that the End-Triassic mass extinction initiated a divergent distribution of growth strategies that persist in present-day archosaurs.

RESULTS

Morphology of BP/1/8484

Both tibiae are large (366 mm in length; Table S1), complete, and well preserved (Figures 1A–1F; see details in STAR Methods). The robust proximal end expands anteroposteriorly and mediolaterally, and the distal end expands mediolaterally to a lesser degree from the shaft. The rugose proximal end of the tibia is subovoid in proximal view (Figure 1E). It bears a horizontally oriented, sigmoidal ridge on the medial surface, forming a broad, "U"-shaped, proximally concave region that faces proximomedially. The shaft is nearly straight and "D"-shaped in cross-section, with the convex portion facing anteriorly. Its middle portion bears a low, raised band of bone that runs from the proximolateral surface to the distomedial surface (Figure 1D). The distal condyles of the tibia are subequal in their distal extent, with a reniform outline in distal view (Figure 1F). The medial condyle is a tab-like structure, and the lateral condyle has a large, posterodistally oriented facet that is subcircular in posterodistal view. This facet is bounded proximally, medially, and laterally by a pronounced lip of bone oriented at approximately 48° to the long axis of the shaft (Figure 1D). The condyles are separated by a depression that runs across the distal surface from anteromedial to posterolateral.

Many characters of the tibia indicate that it pertains to a pseudosuchian archosaur. These include the following: the lack of a cnemial crest, a lateral condyle with a well-developed depression on its proximal surface, and the absence of a distinct posterolateral process on the distal tibia.[14] The general shape of the tibia is similar to that of loricatans, especially the concavity of the proximal end and the sharp division between the distal condyles. The tibia is more robust than those of *Postosuchus* species.[15,16] The posteriorly extensive rugose lip is a common feature in later-branching pseudosuchians, including *Batrachotomus kupferzellensis*,[17] *Dromicosuchus grallator*,[18] *Sphenosuchus acutas*,[10] and *Hesperosuchus agilis*.[14] The distal tibial condyles are subequal in their distal extent, in contrast to *Poposaurus gracilis*,[19] *Postosuchus kirkpatricki*,[15]

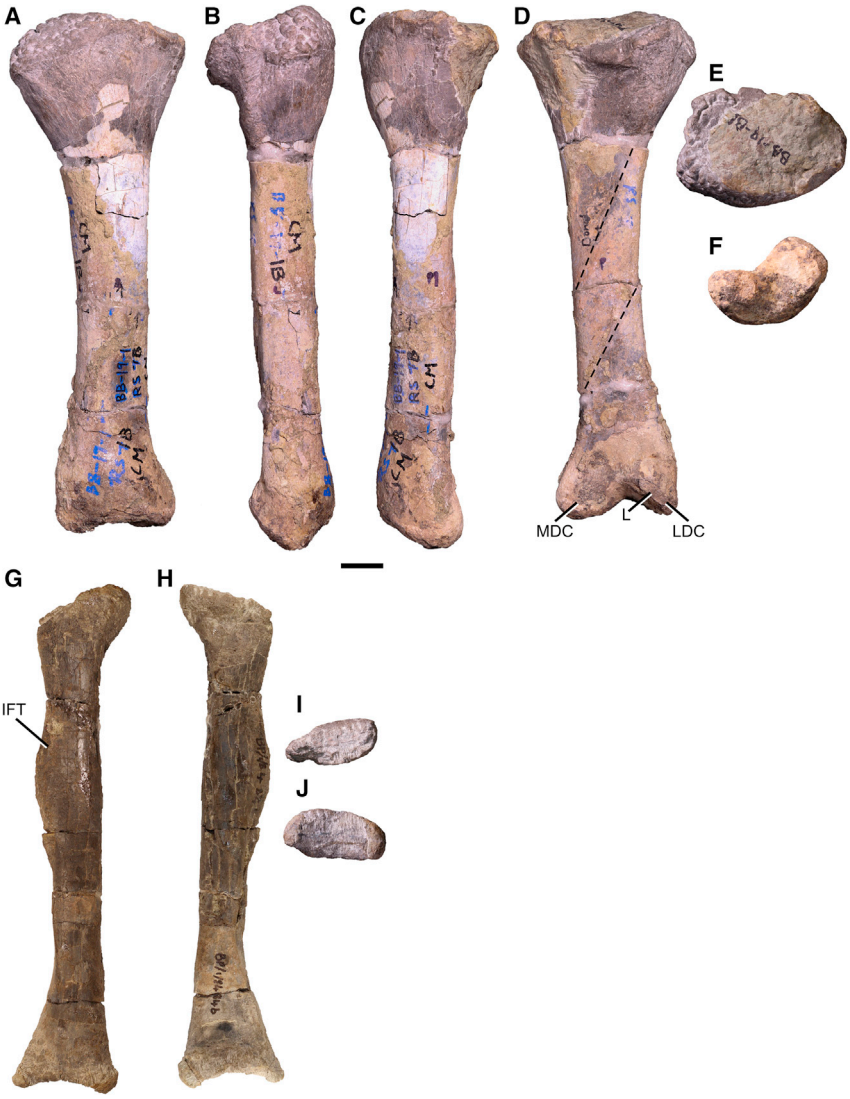

Figure 1. Right tibia and fibula of BP/1/8484
(A–F) Right tibia in (A) anterior, (B) lateral, (C) medial, (D) posterior, (E) proximal, and (F) distal views. (G–J) Right fibula in (G) lateral, (H) medial, (I) proximal, and (J) distal views. Dashed lines indicate diagonal band. Scale bars, 30 mm.
IFT, iliofibularis trochanter; L, lip; LDC, lateral medial condyle; MDC, medial distal condyle.

Hesperosuchus agilis,[14] and *Dromicosuchus grallator*,[18] where the medial condyle projects much farther distally. The angle of the bounding lip of the lateral distal condyle is lower than in most late-branching non-crocodyliform pseudosuchians, for example, *P. kirkpatricki*[2] (60°), *Hesperosuchus agilis*[14] (52°), and *Dromicosuchus grallator*[5] (65°). The diagonal band on the posterior surface of the shaft (Figure 1D) is not present in other pseudosuchian species.

The left fibula is complete and well preserved, with an eroded proximal end (Figures 1G–1J). It is long, straight, and slender, with expanded proximal and distal ends. The proximal end is mediolaterally compressed and anteroposteriorly expanded, and its posterolateral margin meets the posteromedial corner at almost 90° (Figure 1I). A flange-like, mediolaterally compressed iliofibularis trochanter extends along the anterior surface of the shaft and is approximately semicircular in lateral view (Figure 1G). The trochanter begins proximally at ~25% of the shaft length, reaches its maximum anterior width at about 38%, and grades into the diaphysis at 57% of the distance along the shaft, representing ~34% of the total fibula length. The thinner anterior distal condyle expands more than its robust posterior counterpart, which is shallowly concave posteriorly. The concave distal end is subovoid in distal view (Figure 1J). It is bound by a small lip along its lateral and medial margins, and the two distal condyles are subequal in length.

The general shape of the fibula is similar to that of *Dromicosuchus grallator*.[18] The fibula bears one loricatan synapomorphy—the positioning of the iliofibularis trochanter near the midpoint of the bone.[14] This feature is labile among closely related pseudosuchians—the iliofibularis trochanter of BP/1/8484 is on the proximal half of the fibula, as in *Poposaurus gracilis*,[19] *Litargosuchus leptorhynchus* BP/1/5237, and *Dromicosuchus grallator*,[18] but in *Postosuchus kirkpatricki*, it is more distally positioned at the shaft midpoint.[15] The medial surface of the distal portion of the fibula has the banked articular facet seen in later-branching pseudosuchians, such as *Postosuchus kirkpatricki*[15] and *Hesperosuchus agilis*.[14]

When scored in a phylogenetic data matrix aimed at understanding broad archosaurian relationships and heuristically analyzed under the maximum parsimony criterion, BP/1/8484 is recovered in a restricted set of phylogenetic positions close to the origins of Crocodylomorpha (Figure S1).

Osteohistology

The bone tissue of the left tibia of BP/1/8484 (Figure 2A) comprises highly vascularized parallel-fibered bone (PFB) (Figures 2B–2E and S2A–S2F). There is little evidence of secondary remodeling, small resorption cavities are rare (Figures 2C and S2D), and secondary osteons are absent. The PFB tissue contains ellipsoid and flattened, evenly spaced osteocyte lacunae within the intercellular matrix and spindle-shaped osteocyte lacunae in the lamellae surrounding the primary osteons (Figures 2C and 2D). The vascular arrangement is predominantly laminar (Figures 2D and 2E). The presence of three lines of arrested growth (LAGs) indicates temporary cessations in growth. There is a decrease in zone width toward the outer cortex, indicating an overall decrease in growth rate. However, outer circumferential lamellae (OCL) are absent, indicating growth had not ceased (Figures 2E and S2E).

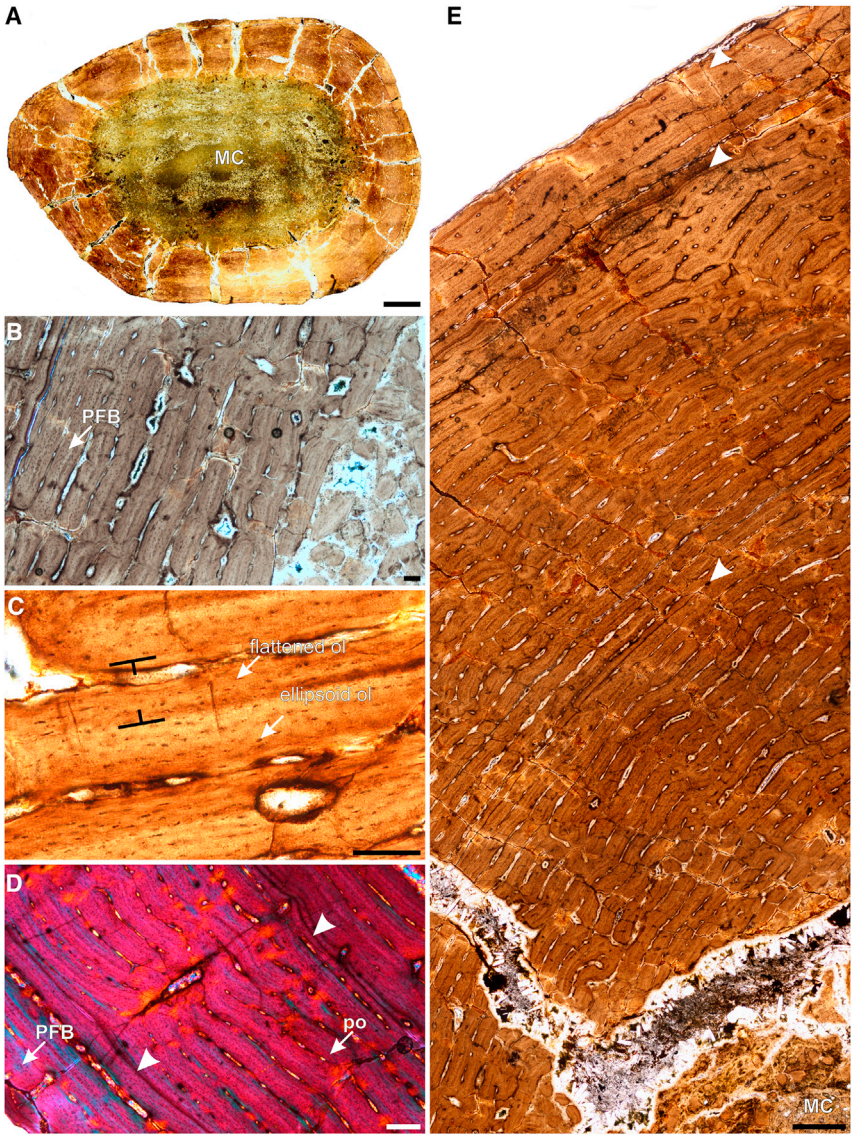

Figure 2. Osteohistology of crocodylomorph BP/1/8484 tibia

(A) Whole cross-section.

(B) Inner cortex of parallel-fibered bone.

(C) Middle cortex showing parallel-fibered bone containing ellipsoid osteocyte lacunae in the intercellular matrix and flattened osteocyte lacunae within the primary osteon (in brackets).
(D) Outer cortex showing moderately vascularized parallel-fibered bone.

(E) Overall cortex showing a decreased spacing between LAGs toward the sub-periosteal surface. Arrowheads indicate growth marks.

Scale bars, 5,000 μm (A), 100 μm (B–D), and 500 μm (E). MC, medullary cavity; ol, osteocyte lacunae; PFB, parallel-fibered bone; PO, primary osteon.

See also Figures S2–S4.

The right fibula of BP/1/8484 (Figure 3A) contains similar bone tissues to those of the tibia (Figures 3B–3F) but with more longitudinally oriented primary osteons. A mid-cortical LAG traverses the bone, but a further three distinct LAGs extend around the outermost cortex. The second and fourth consist of double LAGs (Figures 3B and 3D–3F). The three outermost LAGs are closely spaced but do not form an OCL, indicating a substantial decrease in overall growth rate (Figures 3D–3F) and a subadult stage.

The tibia of *Sphenosuchus* (SAM-PK-3014; Figure S3A) contains highly vascularized longitudinally oriented primary osteons in a woven-parallel complex (Figure S3B) within the first year of growth and thereafter transforms to poorly vascularized lamellar bone tissue toward the subperiosteal surface that may be interpreted as an OCL, except for a small outer region of vascularized bone (Figures S3C and S3D). The slow-growing region contains multiple closely spaced LAGs, but the region of active tissue growth suggests a subadult status. It is probable that *Sphenosuchus* grew larger than this particular specimen. Secondary remodeling in the form of resorption cavities and secondary osteons is absent. A thin layer of endosteal bone tissue lines the medullary cavity.

The *Orthosuchus* tibia (SAM-PK-K409; Figure S3E) contains slowly forming lamellar and PFB interrupted by at least four LAGs. The bone tissue is relatively poorly vascularized, with longitudinally oriented simple canals evenly dispersed throughout the cortex (Figures S3F and S3G). The scan does not provide enough resolution to confirm the presence of primary osteons. Hyper-dense scan regions appear as small white triangles, some of which are associated with osteocyte lacunae (Figure S3G, see red circle). If these represent osteocyte lacunae, combined with the increased vasculature in this region, it suggests that PFB is present here. There is no decrease in the spacing between LAGs toward the subperiosteal surface; consequently, this individual is likely a subadult but still growing slowly.

Three small crocodylomorphs referable to Notochampsoidea (based on their morphological similarity) were sampled for comparison (Figures S4A–S4G). The fibula BP/1/4686 (Figure S4A), tibia of BP/1/8685 (Figures S4B–S4D), and the femur, tibia, and fibula of SAM-PK-K1322 (Figures S4E–S4G) all contain predominantly PFB tissue with predominantly longitudinally oriented simple canals, with some patches of woven bone in tibia BP/1/8685. They likely represent relatively young individuals. Fibula BP/1/4686 does not contain any growth marks, tibia BP/1/8685 and tibia SAM-PK-K1322 each contain two, and the femur and fibula of SAM-PK-K1322 contain one each. The zones between the two growth marks in tibiae BP/1/8685 and SAM-PK-K1322 are narrower than the innermost zone of growth (Figures S4C, S4D, and S4F), indicating a slight decrease in growth rate. BP/1/4686 cannot represent a hatchling of BP/1/8484 as it came from a different part of the formation, and the

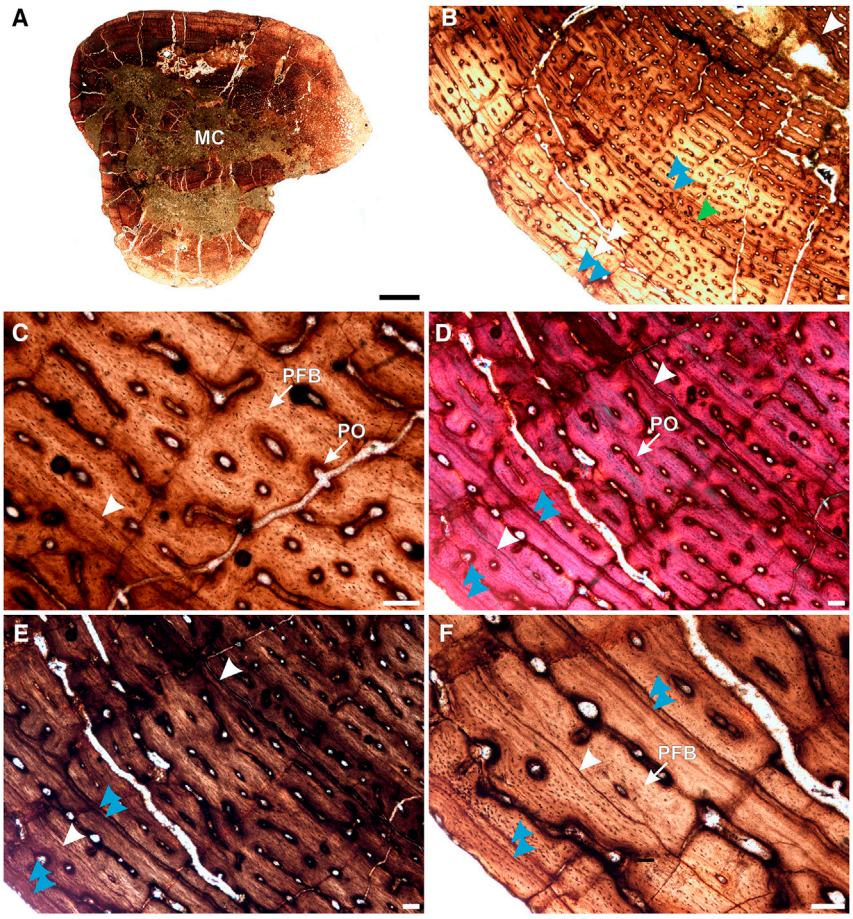

Figure 3. Osteohistology of crocodylomorph BP/1/8484 fibula

(A) Whole cross-section.

(B) Parallel-fibered bone with a laminar vascular arrangement interrupted by LAGs. Green arrowhead indicates a separate LAG in the image but joins the previous double LAG around the rest of the bone.

(C) Showing parallel-fibered bone.

(D) Outer cortex in cross-polarized light showing parallel-fibered bone interrupted by growth marks.

(E) Same in polarized light.

(F) High magnification showing an absence of woven bone and the presence of closely spaced LAGs. Blue arrowheads indicate double LAGs.

Scale bars, 5,000 μm (A) and 100 μm (B–F). MC, medullary cavity; PFB, parallel-fibered bone; PO, primary osteon.

See also Figures S2–S4.

osteohistology indicates that BP/1/8685 and SAM-PK-K1322 are more likely to represent distinct species rather than examples of intraspecific growth variation.

DISCUSSION

Extant crocodilians are ectotherms with slow metabolic and growth rates.[20] This contrasts strongly with the high metabolic and growth rates of their endothermic living sister taxon, birds.[21] Fossil bone histology (osteohistology) surprisingly shows that many stem archosaurs and Triassic pseudosuchians had high rates of bone deposition[6–9,13] and rapid growth rates. Combined with other anatomical evidence from living crocodilians such as four-chambered hearts[1,12] and unidirectional airflow through the lungs,[3] the available data indicate that the slow growth of extant crocodilians reflects a secondary decrease in growth rate, independent of the similar physiological traits seen in other modern reptiles.[1,22]

Many Triassic pseudosuchians sampled so far, including aetosaurs, poposauroids, and rauisuchids, show rapid bone growth (evidenced by a woven-parallel complex) until at least mid-ontogeny.[6,7,9,23] This differs from extant crocodilians, which have slow rates of bone deposition and either parallel-fibered or lamellar bone tissue types,[24,25,26,27,28] with woven-parallel complexes only observed in very young individuals or, rarely, in captive animals raised in optimal growing conditions.[27,29–33]

Slow-growing bone tissues (e.g., lamellar-zonal bone) are also evident among many extinct relatives of extant crocodilians, including most notosuchians and early-diverging neosuchians[34–36] (but see Navarro et al.[37] for different observations in *Notosuchus*), the phylogenetically labile Thalattosuchia, and the small-bodied *Hesperosuchus*.[13] The phylogenetic distribution of these observations suggests that crocodilian-like slow growth originated after the divergences of Poposauroidea or Rauisuchidae from the line leading to Crocodilia and potentially among early crocodylomorphs. If so, then the transition from fast to slow growth rates along the crocodilian stem might have coincided with an evolutionary decrease in body size. However, species with small adult body sizes grow slower and have histological traits characteristic of slow bone deposition,[38,39] raising questions about whether the limited crocodylomorph sample reflects a physiological slowdown or evolutionary body size miniaturization.

Identifying the transition to slow growth on the crocodilian stem lineage is central to explaining the physiological disparity between the two living archosaur groups, crocodilians and birds. The scarcity of osteohistological data for early-branching crocodylomorphs, especially for larger-bodied taxa that lived in the Late Triassic-Early Jurassic, obscures the timing of the shift between rapid bone deposition and high growth rates in early-diverging pseudosuchians[1,7–9,13,23] to slower growth in crocodilians and their closest relatives.[34,35] Understanding this change is relevant regarding the role of physiological traits in relation to survivorship during the End-Triassic mass extinction event (ETE).[40]

The osteohistological data we present here fill this critical knowledge gap, allowing us to refine the timing and nature of this transition (Figure 4). The highly vascularized PFB with a laminar arrangement observed in BP/1/8484 has not previously been found in other pseudosuchians. A similar bone tissue combination was noted recently in the rauisuchian *Prestosuchus*

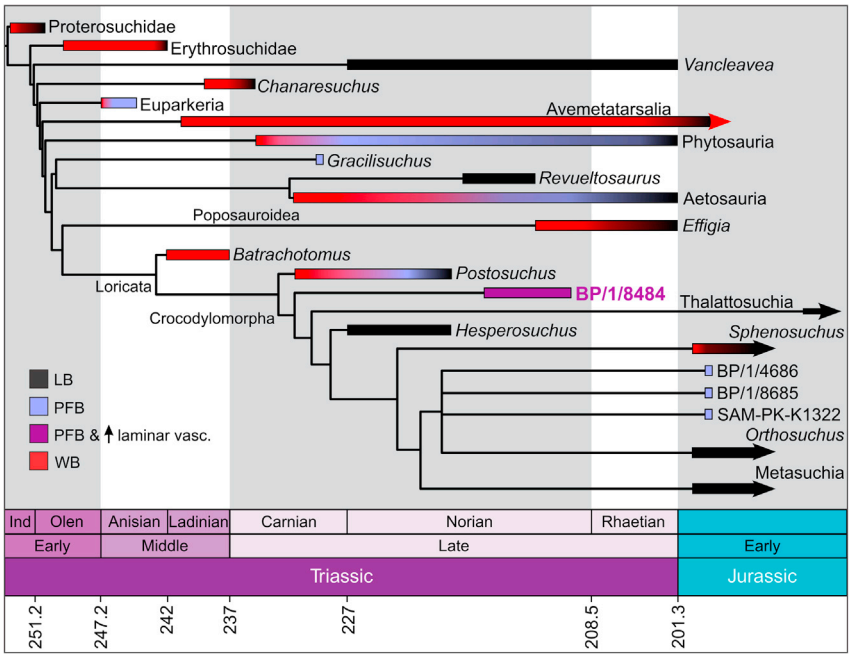

Figure 4. Time-calibrated phylogenetic crocodylomorph tree showing the appearance of slowed growth in the crocodylomorph lineage

Phylogeny based on Nesbitt[14] and Dollman et al.[48]

chiniquensis[41] but contains clear evidence for woven bone as part of a typical woven-parallel complex within the mid-cortex of the humerus and fibula in their study (their Figures 7A–7D). Paradoxically, although the PFB present in BP/1/8484 provides evidence for slower maximum rates of bone growth during mid-ontogeny, its high vascularity is associated with relatively rapid growth rates in other taxa[42] and markedly contrasts with the lamellar-zonal bone indicative of slower growth in smaller-bodied early crocodylomorphs, such as *Hesperosuchus*. This apparent contradiction in growth strategies in BP/1/8484 may be explained by conservation of biomechanical function (laminar vascular orientation), as has been found in several large mammals and sauropod dinosaurs.[43,44] The bone tissue contrasts with the presence of abundant woven bone in the earlier-branching *Batrachotomus*, which indicates rapid growth rates through mid-ontogeny. If the identification of the juvenile *Terrestrisuchus* specimen (VMNH 2374) described by de Ricqlès et al.[6] can be confirmed, it would show that juveniles of early crocodylomorphs were still capable of producing woven bone at very young ages, as in extant crocodilian juveniles (see above). This is supported by our findings from the *Sphenosuchus* tibia, which shows rapid woven bone growth during early ontogeny, which is lost in later ontogenetic stages. Isolated, small patches of woven bone have been cited among some notosuchians, but so far only *Notosuchus* might exhibit a woven-parallel complex into mid-ontogeny[37] (but see Garcia Marsà et al.[36] for a contrasting description).

The comparative anatomy of BP/1/8484 places it phylogenetically close to the base of Crocodylomorpha (Figure 4), suggesting that decreased growth rates arose early in the history of this clade, as hypothesized by Faure-Brac et al.[35] The predominance of PFB in this large-bodied taxon confirms that the slow-growing bone types seen in small adult crocodylomorphs are not a consequence of body size. Later-branching pseudosuchians such as BP/1/8484 are the largest known predators of the late Norian, facing little competition from smaller contemporaneous theropod dinosaurs or cynodonts. The rarity of large-bodied apex predators at this time may have relaxed selection for rapid growth to large body sizes in early crocodylomorphs. Regardless of whether this hypothesis is true, our data suggest that once large predators became more abundant in the Early Jurassic, slow growth rates were already fixed in crocodylomorphs.

Most early-branching crocodylomorphs are hypothesized to have been terrestrial, based on limb proportions and sedimentological observations of their host strata.[1,11,12,45] This differs from the semiaquatic habits of all living and many extinct members of the lineage. Adaptation to semiaquatic habits was previously hypothesized as a driver of decreased growth rates on the crocodilian stem lineage due to lower activity levels and increased reliance on external thermal energy sources in sluggish, semiaquatic ambush predators.[1,11] Our observation that slow-growing tissue types first appeared in gracile-limbed, terrestrial taxa, prior to the transition to semiaquatic lifestyles, directly contradicts this hypothesis and confirms predictions made by Faure-Brac et al.[35] Our results therefore necessitate investigation of alternative explanations for the origin of slow growth in living crocodilians.

Although osteohistology does not provide direct evidence for thermophysiology, it has been used to infer the broader metabolic strategies and body temperatures of extinct species (e.g., Legendre et al.[4,5] and Grigg et al.[46]). Our findings provide critical data that show that the transition to slow growth rates occurred in the Late Triassic (Norian) at the base of Crocodylomorpha (Figure 4). This suggests that the physiology of Late Triassic crocodylomorphs already differed from that of earlier-branching, contemporaneous pseudosuchian lineages. These findings complete the critical knowledge gap laid out by Faure-Brac et al.[35]

By the Early Jurassic, crocodylomorph growth patterns were essentially identical to those of modern-day ectothermic crocodilians. This suggests that decreased metabolic rates were present in crocodylomorphs prior to the ETE and persisted after this biotic crisis. Hypotheses for successful survival strategies across the extinction event must therefore include the possibility that a range of growth characteristics were potentially advantageous, complicating the narrative that high metabolic rates provided competitive advantages to amniote lineages, which has been suggested as an explanation for survival and diversification of dinosaurs during this event.[40,47] Our findings suggest that the ETE acted as a physiological filter, with differential survival of crocodylomorphs with slow and fast growth rates, notably the

extinction of the latter. This led to the earliest Jurassic communities consisting of fast-growing dinosaurs and slow-growing crocodilians, thereby establishing the bimodal distribution of physiological strategies that so clearly differentiates the two living archosaur clades.

STAR★METHODS

Detailed methods are provided in the online version of this paper and include the following:

- KEY RESOURCES TABLE
- RESOURCE AVAILABILITY
  - Lead contact
  - Materials availability
  - Data and code availability
- EXPERIMENTAL MODEL AND SUBJECT DETAILS
  - Geological Context of Specimens
- METHOD DETAILS
  - Phylogenetic analysis
  - Thin Sections
  - Comparative anatomy
  - Institutional Abbreviations

SUPPLEMENTAL INFORMATION

Supplemental information can be found online at https://doi.org/10.1016/j.cub.2023.08.057.

ACKNOWLEDGMENTS

Thank you to Sekhomotso Gubuza for her aid in thin sectioning and to Sginyane Ralane, Themba Jika-Jika, Yoliswa Mei, and the members of the 2019 Qhemegha expedition for their aid during fieldwork. J.B. is supported by the Palaeontological Scientific Trust (PAST). J.B. and J.N.C. are supported by the National Research Foundation (GUN 136513 and 118794, respectively). J.N.C., K.D., and B.M.W. were supported by GENUS: DSI-NRF Centre of Excellence in Palaeosciences. B.M.W. was supported by the P.V. Tobias Education Bursary. P.M.B. was supported by the Science Investment Fund of the Natural History Museum, London.

AUTHOR CONTRIBUTIONS

Conceptualization, J.B., J.N.C., B.M.W., K.D., R.B.J.B., and P.M.B.; investigation, J.B., J.N.C., B.M.W., K.D., R.B.J.B., and P.M.B.; morphological description, B.M.W. and J.N.C.; osteohistological analysis, J.B.; synchrotron scanning, B.M.W., J.N.C., and K.D.; writing, J.B., J.N.C., B.M.W., K.D., R.B.J.B., and P.M.B.

DECLARATION OF INTERESTS

The authors declare no competing interests.

Received: July 6, 2023
Revised: August 8, 2023
Accepted: August 18, 2023
Published: September 14, 2023

REFERENCES

1. Seymour, R.S., Bennett-Stamper, C.L., Johnston, S.D., Carrier, D.R., and Grigg, G.C. (2004). Evidence for endothermic ancestors of crocodiles at the stem of archosaur evolution. Physiol. Biochem. Zool. *77*, 1051–1067.
2. Summers, A.P. (2005). Evolution: warm-hearted crocs. Nature *434*, 833–834. https://doi.org/10.1038/434833a.
3. Farmer, C.G., and Sanders, K. (2010). Unidirectional airflow in the lungs of alligators. Science *327*, 338–340. https://doi.org/10.1126/science.1180219.
4. Legendre, L.J., Segalen, L., and Cubo, J. (2013). Evidence for high bone growth rate in *Euparkeria* obtained using a new paleohistological inference model for the humerus. J. Vertebr. Paleontol. *33*, 1343–1350. https://doi.org/10.1080/02724634.2013.780060.
5. Legendre, L.J., Guénard, G., Botha-Brink, J., and Cubo, J. (2016). Palaeohistological evidence for ancestral high metabolic rate in archosaurs. Syst. Biol. *65*, 989–996. https://doi.org/10.1093/sysbio/syw033.
6. de Ricqlès, A.J., Padian, K., and Horner, J.R. (2003). On the bone histology of some Triassic pseudosuchian archosaurs and related taxa. Ann. Paleontol. *89*, 67–101.
7. de Ricqlès, A., Padian, K., Knoll, F., and Horner, J.R. (2008). On the origin of high growth rates in archosaurs and their ancient relatives: complementary histological studies on Triassic archosauriforms and the problem of a "phylogenetic signal" in bone histology. Ann. Paleontol. *94*, 57–76.
8. Botha-Brink, J., and Smith, R.M.H. (2011). Osteohistology of the Triassic archosauromorphs *Prolacerta*, *Proterosuchus*, *Euparkeria*, and *Erythrosuchus* from the Karoo Basin of South Africa. J. Vertebr. Paleontol. *31*, 1238–1254. https://doi.org/10.1080/02724634.2011.621797.
9. Klein, N., Foth, C., and Schoch, R.R. (2017). Preliminary observations on the bone histology of the Middle Triassic pseudosuchian archosaur *Batrachotomus kupferzellensis* reveal fast growth with laminar fibrolamellar bone tissue. J. Vertebr. Paleontol. *37*, e1333121. https://doi.org/10.1080/02724634.2017.1333121.
10. Walker, A.D. (1990). A revision of *Sphenosuchus acutus* Haughton, a crocodylomorph reptile from the Elliot Formation (Late Triassic or Early Jurassic) of South Africa. Phil. Trans. R. Soc. Lond. B *330*, 1–120. https://doi.org/10.1098/rstb.1990.0185.
11. Colbert, E.H., and Mook, C.C. (1951). The ancestral crocodile *Protosuchus*. Bull. Am. Museum Nat. Hist. *97*, 147–182.
12. Parrish, J.M. (1987). The origin of crocodilian locomotion. Paleobiology *13*, 396–414. https://doi.org/10.1017/S0094837300009003.
13. de Buffrénil, V., de Ricqlès, A.J., Zylberberg, L., and Padian, K. (2021). Skeletal Histology and Paleohistology (CRC Press).
14. Nesbitt, S.J. (2011). The early evolution of archosaurs: relationships and the origin of major clades. Bull. Am. Museum Nat. Hist. *352*, 1–292.
15. Weinbaum, J.C. (2013). Postcranial skeleton of *Postosuchus kirkpatricki* (Archosauria: Paracrocodylomorpha), from the Upper Triassic of the United States. Geological Society, London, Special Publications *379*, 525–553. https://doi.org/10.1144/SP379.7.
16. Peyer, K., Carter, J.G., Sues, H.D., Novak, S.E., and Olsen, P.E. (2008). A new Suchian archosaur from the Upper Triassic of North Carolina. J. Vertebr. Paleontol. *28*, 363–381. https://doi.org/10.1671/0272-4634(2008)28[363:ANSAFT]2.0.CO;2.
17. Gower, D.J., and Schoch, R.R. (2009). Postcranial anatomy of the rauisuchian archosaur *Batrachotomus kupferzellensis*. J. Vertebr. Paleontol. *29*, 103–122. https://doi.org/10.1080/02724634.2009.10010365.
18. Sues, H.-D., Olsen, P.E., Carter, J.G., and Scott, D.M. (2003). A new crocodylomorph archosaur from the Upper Triassic of North Carolina. J. Vertebr. Paleontol. *23*, 329–343. https://doi.org/10.1671/0272-4634(2003)023[0329:ANCAFT]2.0.CO;2.
19. Schachner, E.R., Irmis, R.B., Huttenlocker, A.K., Sanders, K., Cieri, R.L., and Nesbitt, S.J. (2020). Osteology of the Late Triassic bipedal archosaur *Poposaurus gracilis* (Archosauria: Pseudosuchia) from Western North America. Anat. Rec. (Hoboken) *303*, 874–917. https://doi.org/10.1002/ar.24298.
20. Brochu, C.A. (2003). Phylogenetic approaches toward Crocodylian history. Annu. Rev. Earth Planet. Sci. *31*, 357–397.
21. Clarke, A., and Pörtner, H.O. (2010). Temperature, metabolic power and the evolution of endothermy. Biol. Rev. Camb. Philos. Soc. *85*, 703–727. https://doi.org/10.1111/j.1469-185X.2010.00122.x.

22. Cubo, J., and Jalil, N.-E. (2019). Bone histology of *Azendohsaurus laaroussii*: implications for the evolution of thermometabolism in Archosauromorpha. Paleobiology *45*, 317–330. https://doi.org/10.1017/pab.2019.13.

23. Ponce, D.A., Desojo, J.B., and Cerda, I.A. (2023). Palaeobiological inferences of the aetosaur Aetosauroides scagliai (Archosauria: Pseudosuchia) based on microstructural analyses of its appendicular bones. Hist. Biol. *35*, 303–314. https://doi.org/10.1080/08912963.2022.2035728.

24. de Ricqlès, A. (1976). On bone histology of fossil and living reptiles, with comments on its functional and evolutionary significance. In Morphology and Biology of Reptiles, A.d'A. Bellairs, and C.B. Cox, eds. (Academic Press), pp. 123–150.

25. Woodward, H.N., Horner, J.R., and Farlow, J.O. (2011). Osteohistological evidence for determinate growth in the American alligator. J. Herpetol. *45*, 339–342. https://doi.org/10.1670/10-274.1.

26. Lee, A.H. (2004). Histological organization and its relationship to function in the femur of *Alligator mississippiensis*. J. Anat. *204*, 197–207. https://doi.org/10.1111/j.0021-8782.2004.00275.x.

27. Woodward, H.N., Horner, J.R., and Farlow, J.O. (2014). Quantification of intraskeletal histovariability in *Alligator mississippiensis* and implications for vertebrate osteohistology. PeerJ *2*, e422. https://doi.org/10.7717/peerj.422.

28. Botha-Brink, J., Bento Soares, M.B., and Martinelli, A.G. (2018). Osteohistology of Late Triassic prozostrodontian cynodonts from Brazil. PeerJ *6*, e5029. https://doi.org/10.7717/peerj.5029.

29. Reid, R.E.H. (1984). Primary bone and dinosaurian physiology. Geol. Mag. *121*, 589–598. https://doi.org/10.1017/S0016756800030739.

30. Reid, R.E.H. (1997). Dinosaurian physiology: the case for ''intermediate'' dinosaurs. In The Complete Dinosaur, J.O. Farlow, and M.K. Brett-Surman, eds. (Indiana University Press), pp. 449–473.

31. Chinsamy, A., and Hillenius, W.J. (2004). Physiology of non-avian dinosaurs. In The Dinosauria, D.B. Weishampel, P. Dodson, and H. Osmólska, eds. (University of California Press), pp. 643–659.

32. Padian, K., Horner, J.R., and de Ricqlès, A. (2004). Growth in small dinosaurs and pterosaurs: the evolution of archosaurian growth strategies. J. Vertebr. Paleontol. *24*, 555–571. https://doi.org/10.1671/0272-4634(2004)024[0555:GISDAP]2.0.CO;2.

33. Tumarkin-Deratzian, A.R. (2007). Fibrolamellar bone in wild adult *Alligator mississippiensis*. J. Herpetol. *41*, 341–345. https://doi.org/10.1670/0022-1511(2007)41[341:FBIWAA]2.0.CO;2.

34. Cubo, J., Sena, M.V.A., Aubier, P., Houee, G., Claisse, P., Faure-Brac, M.G., Allain, R., Andrade, R.C.L.P., Sayão, J.M., and Oliveira, G.R. (2020). Were Notosuchia (Pseudosuchia: Crocodylomorpha) warm-blooded? A palaeohistological analysis suggests ectothermy. Biol. J. Linn. Soc. *131*, 154–162. https://doi.org/10.1093/biolinnean/blaa081.

35. Faure-Brac, M.G., Amiot, R., de Muizon, C., Cubo, J., and Lécuyer, C. (2022). Combined paleohistological and isotopic inferences of thermometabolism in extinct Neosuchia, using *Goniopholis* and *Dyrosaurus* (Pseudosuchia: Crocodylomorpha) as case studies. Paleobiology *48*, 302–323. https://doi.org/10.1017/pab.2021.34.

36. Garcia Marsà, J.A., Martinelli, A.G., Lio, G., Nava, W., and Novas, F.E. (2022). Bone microstructure in terrestrial Mesozoic Crocodylomorpha: *Neuquensuchus* and notosuchians. Lethaia *55*, 1–11. https://doi.org/10.18261/let.55.3.6.

37. Navarro, T.G., Cerda, I.A., and Pol, D. (2023). Microstructural characterization and growth dynamics in *Notosuchus terrestris*, a Mesoeucrocodylia crocodyliform from the Upper Cretaceous of Northern Patagonia, Argentina. Cret. Res. *150*, https://doi.org/10.1016/j.cretres.2023.105607.

38. Case, T.J. (1978). Speculations on the growth rate and reproduction of some dinosaurs. Paleobiology *4*, 320–328. https://doi.org/10.1017/S0094837300006023.

39. Erickson, G.M., Rauhut, O.W.M., Zhou, Z., Turner, A.H., Inouye, B.D., Hu, D., and Norell, M.A. (2009). Was dinosaurian physiology inherited by birds? Reconciling slow growth in *Archaeopteryx*. PLoS One *4*, e7390. https://doi.org/10.1371/journal.pone.0007390.

40. Olsen, P.E., Kent, D.V., Sues, H.D., Koeberl, C., Huber, H., Montanari, A., Rainforth, E.C., Fowell, S.J., Szajna, M.J., and Hartline, B.W. (2002). Ascent of dinosaurs linked to an iridium anomaly at the Triassic-Jurassic boundary. Science *296*, 1305–1307. https://doi.org/10.1126/science.1065522.

41. Ponce, D.A., Scheyer, T.M., Cerda, I.A., and Desojo, J.B. (2023). Palaeobiological inferences of ''rauisuchians'' *Fasolasuchus tenax* (Los Colorados Fm., Argentina) and *Prestosuchus chiniquensis* (Santa Maria Super sequence, Brazil) from the Middle-Upper Triassic of South America based on microstructural analyses. J. Anat. 1–17. 10.1111/joa.13937. https://doi.org/10.1111/joa.13937.

42. Amprino, R. (1947). La structure du tissue osseux envisage comme expression de differences dans la vitesse de l'accroissement. Arch. Biol. *58*, 315–330.

43. Margerie de, E., Robin, J.P., Verrier, D., Cubo, J., Groscolas, R., and Castanet, J. (2004). Assessing a relationship between bone microstructure and growth rate: a fluorescent labelling study in the king penguin chick (Aptenodytes patagonicus). J. Exp. Biol. *207*, 869–879. https://doi.org/10.1242/jeb.00841.

44. Stein, K., and Prondvai, E. (2014). Rethinking the nature of fibrolamellar bone: an integrative biological revision of sauropod plexiform bone formation. Biol. Rev. Camb. Philos. Soc. *89*, 24–47. https://doi.org/10.1111/brv.12041.

45. Walker, A.D. (1972). New light on the origin of birds and crocodiles. Nature *237*, 257–263. https://doi.org/10.1038/237257a0.

46. Grigg, G., Nowack, J., Bicudo, J.E.P.W., Bal, N.C., Woodward, H.N., and Seymour, R.S. (2022). Whole-body endothermy: ancient, homologous and widespread among the ancestors of mammals, birds and crocodylians. Biol. Rev. Camb. Philos. Soc. *97*, 766–801. https://doi.org/10.1111/brv.12822.

47. Bakker, R.T. (1972). Anatomical and ecological evidence of endothermy in dinosaurs. Nature *238*, 81–85. https://doi.org/10.1038/238081a0.

48. Dollman, K.N., Clark, J.M., Viglietti, P.A., Browning, C., and Choiniere, J.N. (2021). Revised anatomy, taxonomy and biostratigraphy of *Notochampsa istedana* Broom, 1904, a Lower Jurassic crocodyliform from the Clarens Formation (Stormberg Group), and its implications for early crocodyliform phylogeny. J. Syst. Palaeontol. *19*, 651–675. https://doi.org/10.1080/14772019.2021.1948926.

49. Viglietti, P.A., McPhee, B.W., Bordy, E.M., Sciscio, L., Barrett, P.M., Benson, R.B.J., Wills, S., Tolchard, F., and Choiniere, J.N. (2020). Biostratigraphy of the *Scalenodontoides* assemblage zone (Stormberg Group, Karoo Supergroup), South Africa. S. Afr. J. Geol. *123*, 239–248. https://doi.org/10.25131/sajg.123.0017.

50. Bordy, E.M., Abrahams, M., Sharman, G.R., Viglietti, P.A., Benson, R.B.J., McPhee, B.W., Barrett, P.M., Sciscio, L., Condon, D., Mundil, R., et al. (2020). A chronostratigraphic framework for the upper Stormberg Group: implications for the Triassic-Jurassic boundary in southern Africa. Earth Sci. Rev. *203*, 103120. https://doi.org/10.1016/j.earscirev.2020.103120.

51. Butler, R.J., Sullivan, C., Ezcurra, M.D., Liu, J., Lecuona, A., and Sookias, R.B. (2014). New clade of enigmatic early archosaurs yields insights into early pseudosuchian phylogeny and the biogeography of the archosaur radiation. BMC Evol. Biol. *14*, 128. https://doi.org/10.1186/1471-2148-14-128.

52. Cau, A., Beyrand, V., Voeten, D.F.A.E., Fernandez, V., Tafforeau, P., Stein, K., Barsbold, R., Tsogtbaatar, K., Currie, P.J., and Godefroit, P. (2017). Synchrotron scanning reveals amphibious ecomorphology in a new clade of bird-like dinosaurs. Nature *552*, 395–399.

53. Carlson, K.J., Stout, D., Jashashvili, T., de Ruiter, D.J., Tafforeau, P., Carlson, K., and Berger, L.R. (2011). The endocast of MH1, *Australopithecus sediba*. Science *333*, 1402–1407.

54. Mirone, A., Brun, E., Gouillart, E., Tafforeau, P., and Kieffer, J. (2014). The PyHST2 hybrid distributed code for high speed tomographic reconstruction with iterative reconstruction and a priori knowledge capabilities. Nucl. Instrum. Methods Phys. Res. B *324*, 41–48.

55. Paganin, D., Mayo, S.C., Gureyev, T.E., Miller, P.R., and Wilkins, S.W. (2002). Simultaneous phase and amplitude extraction from a single defocused image of a homogeneous object. J. Microsc. *206*, 33–40.

56. Smith, T.M., Tafforeau, P., Le Cabec, A., Bonnin, A., Houssaye, A., Pouech, J., Moggi-Cecchi, J., Manthi, F., Ward, C., Makaremi, M., et al. (2015). Dental ontogeny in Pliocene and early Pleistocene hominins. PLoS One *10*, e0118118.

57. Schneider, C.A., Rasband, W.S., and Eliceiri, K.W. (2012). NIH Image to ImageJ: 25 years of image analysis. Nat. Methods *9*, 671–675. https://doi.org/10.1038/nmeth.2089.

STAR★METHODS

KEY RESOURCES TABLE

REAGENT or RESOURCE	SOURCE	IDENTIFIER
Biological samples		
Crocodylomorph osteohistological thin sections	Evolutionary Studies Institute, University of the Witwatersrand	Cat#BP/1/8484; 4686; 8685
Crocodylomorph osteohistological thin sections	Iziko Museums of South Africa	Cat#SAM-PK-K1322

RESOURCE AVAILABILITY

Lead contact

Further information and requests for resources or protocol details should be directed to and will be fulfilled by the lead contact, Jennifer Botha (jennifer.botha1@wits.ac.za).

Materials availability

The thin-sections generated from this study are currently housed at the Evolutionary Studies Institute, University of the Witwatersrand.

Data and code availability

- Any additional information required to reanalyze the data reported in this study is available from the lead contact upon request.
- All raw data is available in the supplemental information or is publicly available in existing publications.
- This paper does not report original code.

Any additional information required to reanalyze the data reported in this paper is available from the lead contact upon request.

EXPERIMENTAL MODEL AND SUBJECT DETAILS

Geological Context of Specimens

The discovery of a new species of large-bodied (see Table S1 for comparative measurements), early-branching crocodylomorph (BP/1/8484) from Qhemegha Village in the Eastern Cape Province of South Africa, prompted this study. BP/1/8484 was found ex-situ but associated in the float from a multi-taxon bonebed in the lower half of the lower Elliot Formation, situated within the *Scalenodontoides* Assemblage Zone.[49] The specimen includes a left tibia and a right tibia and fibula, which are readily distinguishable from the sauropodomorph and theropod dinosaur remains in the bonebed. Litho- and biostratigraphic comparisons with well-dated nearby strata indicate that BP/1/8484 is Late Triassic (Norian) in age.[50] We compared the morphology to other Crocodylomorpha and the osteohistology to several other small crocodylomorph specimens referrable to Notochampsoidea collected from Lower Jurassic strata, as well as *Sphenosuchus acutus* and *Orthosuchus stormbergi* from the Early Jurassic upper Elliot Formation of South Africa.

METHOD DETAILS

Phylogenetic analysis

To assess the phylogenetic position of BP/1/8484, we scored it as an OTU in the phylogenetic data matrix of Butler et al.[51] This matrix is aimed at understanding relationships among archosaurs, particularly pseudosuchian higher phylogenetic relationships and contains a sufficient taxon sample to adequately test the position of the new specimen among them. We were able to score 18 total characters for the tibia and fibula (out of 413 total characters). Using the resulting matrix of 85 taxa and 413 characters, we searched for most-parsimonious tree (MPT) topologies using TNT v.1.6 and the following search settings: hold up to 10,000 trees; conduct 1000 random addition of sequences (Wagner builds) with a random seed of 1; hold up to 1 tree per replicate; search using TBR. We submitted the MPTs from that analysis protocol to an additional round of TBR swapping holding up to 10000 topologies. Our results show that BP/1/8484 can hold multiple most-parsimonious positions, but only at a restricted set of nodes (see Figure S1), summarized here:

- As sister taxon to or among early branches of Crocodylomorpha
- As a rauisuchid (either sister to *Rauisuchus* or *Postosuchus*)
- As sister to the clade comprising Rauisuchidae + Crocodylomorpha.

Character scores for BP/1/8484 following Butler et al.[51]

???0010000001001101 10???

Thin Sections

The thin-sectioning was conducted at the National Museum, Bloemfontein using similar techniques to those described in Botha-Brink et al.[28] Transverse sections were taken from the mid-diaphysis from all elements as far as possible. Given that there was enough material, a section from the mid-diaphysis/metaphysis was also taken from the tibia and sectioned in longitudinal section for further analysis. The left tibia and right fibula were sectioned for osteohistological analysis. These thin-sections were compared with those from the other small notochampsoid specimens: the fibula of BP/1/4686; the tibia of BP/1/8685; and the femur, tibia and fibula of SAM-PK-K1322. Propagation phase contrast Synchrotron X-ray micro-Computed Tomography was used to achieve virtual histological thin sections at the European Synchrotron and Radiation Facility (Grenoble, France) on BM05 (10.15151/ESRF-ES-817601169). We obtained scans for *Sphenosuchus acutus* (tibia; SAM-PK-3014) and *Orthosuchus stormbergi* (tibia; SAM-PK-K409) at the midshaft of each bone. The beamline setup was for propagation phase-contrast synchrotron X-ray micro-computed tomography with a polychromatic beam of 97.8 keV, with molybdenum (0.95mm) and copper (1.18mm) attenuator filters, a 500nm thick luAg scintillator, a sample-detector distance of 1.4 metre, and a voxel size of 2.42μm. We used a PCO edge 4,2 sCMOS (PCO, Kelheim Germany), recording 9900 projections with a total exposure time of 30ms, with three accumulated images of 10ms.[52] The centre of rotation was shifted to near the edge of the field of view (half-acquisition mode), to increase the size of the reconstructed images.[53] The final tomographic volume was reconstructed using PyHST2[54] and the single distance Paganin phase retrieval approach.[55] All histological thin sections were realised in VG (Volume Graphics, Heidelburg, Germany) using a protocol established by Smith et al.[56] The tibia and fibula of BP/1/8484 were moulded and cast before a piece was removed from each element for thin-sectioning. Osteohistological terminology follows that of de Buffrénil.[13]

Comparative anatomy

The morphological descriptions were done with personal inspection of the specimens and reference to the published literature. Linear measurements were taken with a Mitutoyo digimatic caliper (model: CD-6''C, Aurora, [IL], US) and angular measurements were taken using ImageJ[57] on high-resolution digital photographs in orthogonal viewing planes. We employ non-standard Romerian terminology for our anatomical observations (e.g., anterior/posterior rather than rostral/caudal). We use the descriptive terms "long/short", "tall/low", and "broad/narrow" to describe variation in the anteroposterior, dorsoventral, and mediolateral directions, respectively.

The complete right tibia (Figures 1A–1F) is broken in three places along the shaft, but it is otherwise missing only small fragments of its cortical surface. The proximal end of the left tibia is weathered, and its cortical surface is slightly eroded. The distal end of the left tibia has a small fragment of rib adhering to its posterior surface, obscuring the view of the medial facet. In general, the tibia has a robust proximal end that is expanded anteroposteriorly and mediolaterally. Its shaft is straight with only slight medial bowing. The distal end is less expanded than the proximal end, and the expansion is primarily in the mediolateral direction (Figures 1B and 1C).

The proximal end of the tibia is subovoid in proximal view and has a rugose proximal surface bearing numerous small bumps and pits (Figure 1E). This rugose surface extends onto the proximalmost end of the lateral side of the anterior surface for a short distance, where it is bounded by a low lip of bone that forms an encircling margin between the proximal surface and the shaft. The anterolateral quarter of the proximal surface is convex, the anteromedial quarter is shallowly concave and slopes medially, the posteromedial quarter is flat, and the posterolateral quarter is deeply concave, sloping into a distinct subcircular area that forms the lateral side of the fibular facet. The anterior surface of the proximal end is smooth and highly convex. A pennate array of faint striations is present on its cortical surface, which splay proximolaterally and proximomedially, and converge at the junction with the shaft as they extend distally. The most conspicuous feature of the medial surface of the proximal end is a horizontally oriented, sigmoidal ridge that marks the junction with the proximal surface. This sigmoidal feature makes a broad, 'U'-shaped, proximally concave region that faces proximomedially, which is in turn bordered posteriorly by a proximally convex margin along the fibular condyle. The border between the medial and posterior surfaces is marked by a proximodistally extending ridge that grades into the fibular condyle proximally and into the shaft distally at the level of the proximal expansion. The posterior surface of the proximal end is bounded proximomedially by the fibular condyle, and proximally by a mediolaterally broad, posteriorly extensive rugose lip that is deeply concave proximally. Distal to this lip, the posterior surface is flat. The lateral surface of the proximal end is strongly convex and rugose, bearing a low, proximodistally extending ridge along its posterior margin and a large, rugose, hemispherical tubercle on its anteroproximal margin. Distal to these features, the surface is smooth and convex, and grades into the tibial shaft (Figure 1).

The tibial shaft is almost 'D'-shaped in cross-section, with the convex portion facing anteriorly and the flat portion facing posteriorly. The entire anterior surface of the shaft is convex mediolaterally, extending onto the anterior surface of the distal condyles. The lateral boundary between the anterior surface and the posterior surface is marked by a low ridge that is subtriangular in cross-section, and that extends proximodistally from the expanded proximal end to the distal condyles. The proximal and distal ends of the posterior surface are flat, but the middle portion bears a low, raised band of bone that runs diagonally from the proximolateral surface to the distomedial surface of the shaft (Figure 1D).

The distal end of the tibia (Figure 1F) is slightly expanded medially and laterally, and the distal condyles are subequal in their distal extent. In distal view, the condyles have a reniform outline, with the anterior margin smoothly convex, the posterior margin concave, the medial margin bulbous, and the lateral margin bearing a laterally directed point that forms the distalmost extent of the low ridge along the shaft. The medial condyle is a tab-like structure that extends distomedially. It is flat on the posterior and distal surfaces, and its medial surface is convex. The lateral condyle has a large, conspicuous facet that is subcircular in posterodistal view and which is oriented strongly posterodistally. This facet is bounded proximally, medially, and laterally by a pronounced lip of bone. In particular, the proximolateral margin of this lip is oriented at approximately 48° to the long axis of the shaft. The condyles are separated by a concave depression that runs diagonally across the distal surface from the anteromedial side to the posterolateral side.

The left fibula (Figures 1G–1J) is well preserved and is nearly complete with the exception of the proximal end, which is weathered (Figures 1G and 1H). The anteroproximal portion of the proximal end is weathered away at a roughly 45° to the rest of the bone. The shaft is mediolaterally crushed with an artificial longitudinal depression along its posterior surface. In general, the fibula is a long, straight, and slender bone with expanded proximal and distal ends.

The proximal end of the fibula (Figure 1I) is mediolaterally compressed. In proximal view, the posterolateral margin of the proximal end is rounded until it meets the posteromedial corner at almost 90°. The medial margin is generally straight in proximal view. The anterior portion of the proximal end is badly eroded and medial and lateral margins taper to a point anteriorly. The proximal end tapers towards the shaft gently and slightly on the anterior side of the proximal end, but more abruptly on the posterior side after a prominent expansion. This expansion points proximoposteriorly at 45° to the shaft. The proximal expansion does not appear to be part of a general curve of the bone but rather a discrete feature limited to the proximal end.

The most prominent feature of the shaft is the iliofibularis trochanter (Figure 1G), a prominent mediolaterally compressed flange that extends along the anterior surface of the shaft and is approximately semicircular in lateral view. The trochanter has a total length of 122 mm, representing ~34% of the total fibula length. The distal end of the shaft expands anteriorly more than it does on the posterior side, creating a more prominent anterior condyle.

In distal view, the distal end is subovoid in outline and its distal surface is concave (Figure 1J). The distal surface is bound by a small lip along its lateral and medial margins. The medial surface is crushed inwards just below this lip. The two distal condyles of the fibula are subequal in length. The anterior condyle is thinner and has a straighter anterior surface compared to the more robust posterior condyle which is shallowly concave posteriorly.

The posterior expansion of the proximal end is a pseudosuchian character seen in almost all crocodile-line archosaurs.[1] However, the posterior expansion is unlike that seen in *Dromicosuchus grallator*[5] which appears to be part of the general curvature of the bone. The fibula is also similar to later branching pseudosuchians such as *Postosuchus kirkpatricki*[2] and *Hesperosuchus agilis*[1] where the medial surface of the distal portion of the element has a banked articular facet.

Institutional Abbreviations

AMNH, American Museum of Natural History, New York, New York, United States; BP, Evolutionary Studies Institute, University of the Witwatersrand, Johannesburg, South Africa; MNS, Staatliches Museum für Naturkunde, Stuttgart, Germany; PEFO, Petrified Forest National Park, Arizona, United States; PVL, Paleontología de Vertebrados, Instituto Miguel Lillo, Tucumán, Argentina; SAM-PK, Iziko South African Museum, Cape Town, South Africa; SNSB-BSPG, Staatlich Naturwissenschaftliche Sammlungen Bayerns, Bayerische Staatssammlung für Paläontologie und Geologie, Munich, Germany; TTU, Museum of Texas Tech University, Lubbock, Texas, United States; UNC, University of North Carolina, Chapel Hill, North Carolina, United States; YPM, Yale Peabody, New Haven, Connecticut, United States.